Pis'ma v ZhETF, vol. 106, iss. 10, pp. 642 – 643

Microstructural properties and evolution of nanoclusters in liquid Si during rapid cooling process

T. Gao[1)], *X. Hu, Y. Li, Z. Tian, Q. Xie*[1)], *Q. Chen, Y. Liang, X. Luo, L. Ren, J. Luo*

Guizhou Provincial Key Laboratory of Public Big Data, Institute of New Type Optoelectronic Materials and Technology, College of Big Data and Information Engineering, Guizhou University, 550025 Guiyang, China

Submitted 3 August 2017
Resubmitted 12 October 2017

DOI: 10.7868/S0370274X1722009X

The wide-ranging applications of amorphous silicon (a-Si) are attracting considerable attention from structural researchers [1–6]. Considering that the macroscopic properties of Si are mainly determined by its microstructures, detailed structural information at the atomic level during its formation processes must be obtained. Although many structural models of liquid Si (l-Si) and a-Si have been established [7–10], adequate identification of the realistic structural features of a-Si remains difficult [11, 12].

Computer simulations are powerful tools for understanding the role of a short-range order in a disordered network. The two- and three-body empirical Stillinger–Weber (SW) potential [13], the Tersoff empirical model potential [14, 15], as well as the two- and three-body classical inter-atomic potentials of Biswas and Hamann [16] have been proposed to describe the interaction between atoms in l-Si and a-Si in computer simulations. Among them, the Stillinger–Weber potential is widely used for l-Si and a-Si simulations [13, 17, 18].

Accurate methods are needed for the quantitative clarification of microstructures. Many structural analysis methods exist, such as the Bernal polyhedron [19], Honeycutt–Andersen index[20], Cluster Type Index method [21, 22], and Voronoi polyhedron method [23, 24]. Voronoi polyhedron index is introduced to describe the microstructures during cooling process of Si, because this model can provide a better representation on the nearest-neighbor shell of l-Si, a-Si and crystalline Si (c-Si).

The previous researches pay more attentions on the crystallization [25–27], the network structures [28, 29], and the nanoparticles of a-Si [30]. In this paper, we mainly focus on the structural properties and evolutions of nanocluster in Si at the atomic level during its rapid quenching process and this work helps understand a-Si networks and the stacking model of polyhedron in l-Si.

1)e-mail: gaotinghong@sina.com; qxie@gzu.edu.cn

In this study, l-Si and a-Si are simulated by MD simulation techniques using the SW potential [18]. MD simulation was carried out in a cubic box under periodic boundary conditions with 8000 Si particles by using LAMMPS [31]. The simulations were performed in the NPT ensemble with zero pressure and the time step of 1.0 fs. First, the system runs 40000 time steps at 2700 K to guarantee an equilibrium liquid state. Then, the temperature gradually decreases to 200 K with a cooling rate of 10^{12} K/s. The configurations were recorded with intervals of 100 K during the quenching process. The RDF and Voronoi polyhedron method were used to analyze the structures of l-Si and a-Si.

The a-Si formed around 800 K and short-range structures have been enhanced during solidification. The $\langle 2\,3\,0\,0 \rangle$ and $\langle 4\,0\,0\,0 \rangle$ polyhedrons are two important polyhedrons in Si during the quenching process. They affect the local structures by their different positions and connection modes. However, others such as $\langle 0\,6\,0\,0 \rangle$, $\langle 2\,2\,2\,0 \rangle$, and $\langle 0\,5\,2\,0 \rangle$ can maintain their structures only at high temperatures and are very rare at low temperatures.

The $\langle 0\,6\,0\,0 \rangle$, $\langle 2\,2\,2\,0 \rangle$, and $\langle 0\,5\,2\,0 \rangle$ polyhedrons tend to be transform into the $\langle 4\,0\,0\,0 \rangle$ and $\langle 2\,3\,0\,0 \rangle$ polyhedrons. The $\langle 4\,0\,0\,0 \rangle$ polyhedrons can link with others to form nanoclusters. Tetrahedrons often tend to involve distortion connections and deviate from the ideal position. The different connection modes of polyhedrons determine the variety of the local structures in amorphous and liquid Si.

Fig. 1 shows that the cluster tends to be regular, although this cluster is slightly distorted. This nanocluster involves five $\langle 2\,3\,0\,0 \rangle$ and seventeen $\langle 4\,0\,0\,0 \rangle$ polyhedrons. Although a large number of $\langle 4\,0\,0\,0 \rangle$ polyhedrons emerge in this cluster, the neighboring atoms deviate from the ideal position. The $\langle 2\,3\,0\,0 \rangle$ polyhedron has five neighboring atoms that destroy the translational symmetry of the crystal structure. During the crystallization process, atoms need a certain time to adjust their own positions and achieve the ideal lattice position. Conse-

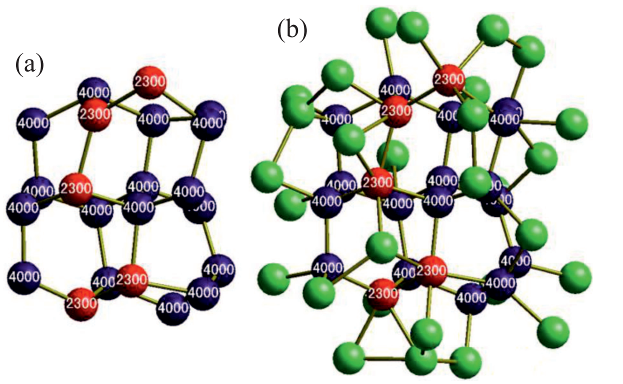

Fig. 1. (Color online) A nanocluster with their Voronoi polyhedron index in Si at 200 K. (a) – Crystalline Si cluster, (b) – cluster and its neighbors

quently, this crystal cluster cannot evolve to a crystal structure because of the high cooling rate of 10^{12} K/s.

Full text of the paper is published in JETP Letters journal. DOI: 10.1134/S0021364017220015

1. M. M. J. Treacy and K. B. Borisenko, Science **335**, 950 (2012).
2. P. L. Tereshchuk, Z. M. Khakimov, F. T. Umarova, and M. T. Swihart, Phys. Rev. B **76**, 125418 (2007).
3. Z. Liu, J. Wen, T. Zhou, Ch. Xue, Yu. Zuo, Ch. Li, B. Cheng, and Q. Wang, Thin Solid Films **597**, 39 (2015).
4. K. O. Hara, C. T. Trinh, Y. Kurokawa, K. Arimoto, J. Yamanaka, K. Nakagawa, and N. Usami, Thin Solid Films **636**, 546 (2017).
5. S. Hui, H. C. Wu, S. C. Chen, H. Sun, H.-Ch. Wu, Sh.-Ch. Chen, C.-W. Ma, and L. X. Wang, Nanoscale Research Letters **12**(1), 224 (2017).
6. X. Chen, B. H. Jia, J. K. Saha, B. Y. Cai, N. Stokes, Q. Qiao, Y. Q. Wang, Z. R. Shi, and M. Gu, Nano Lett. **12**(5), 2187 (2012).
7. F. Wooten, K. Winer, and D. Weaire, Phys. Rev. Lett. **54**, 1392 (1985).
8. I. Štich, R. Car, and M. Parrinello, Phys. Rev. B **44**, 11092 (1991).
9. R. Biswas, B. C. Pan, and Y. Y. Ye, Phys. Rev. Lett. **88**, 205502 (2002).
10. M. M. J. Treacy and K. B. Borisenko, Science **335**, 950 (2012).
11. A. Pedersen, L. Pizzagalli, and H. Jónsson, New J. Phys **19**, 063018 (2017).
12. M. J. Cliffe, A. P. Bartók, R. N. Kerber, C. P. Grey, G. Csányi, and A. L. Goodwin, Phys. Rev. B **95**, 224108 (2017).
13. F. H. Stillinger and T. A. Weber, Phys. Rev. B **31**, 5262 (1985).
14. J. Tersoff, Phys. Rev. Lett. **56**, 632 (1986).
15. J. Tersoff, Phys. Rev. B **38**, 9902 (1988).
16. R. Biswas and D. R. Hamann, Phys. Rev. B **36**, 6434 (1987).
17. B. P. Feuston, R. K. Kalia, and P. Vashishta, Phys. Rev. B **35**, 6222 (1987).
18. M. Ishimaru, K. Yoshida, and T. Motooka, Phys. Rev. B **53**, 7176 (1996).
19. J. Bernal, Nature **183**(17), 141 (1959).
20. J. D. Honeycutt and H. C. Anderson, J. Phys. Chem. **91**(19), 4950 (1987).
21. R. S. Liu, K. J. Dong, and Z. A. Tian, J. Phys.: Condens. Matter **19**(19), 196103 (2007).
22. R. S. Liu, K. J. Dong, and J. Y. Li, J. Non-Cryst. Solids **351**(6–7), 612 (2005).
23. J. L. Finney, Proc. R. Soc. London, Ser. A **319**, 479 (1970).
24. H. W. Sheng, W. K. Luo, F. M. Alamgir, J. M. Bai, and E. Ma, Nature (London) **439**, 419 (2006).
25. G. R. Chen, C. Song, J. Xu, D. Q. Wang, L. Xu, and Z. Y. Ma, Acta Physica Sinica **59**(8), 5681 (2010).
26. S. Munetoh, P. X. Yan, T. Ogata, T. Motooka, and R. Teranishi, Transactions of the Iron & Steel Institute of Japan **50**(12), 1925 (2010).
27. S. Maruyama and K. Teshima, The Japan Society of Mechanical Engineers **2002**, 31 (2002).
28. I. H. Lee and K. J. Chang, Phys. Rev. B Condens. Matter **50**(24), 18083 (1994).
29. D. A. Drabold, P. A. Fedders, O. F. Sankey, and J. D. Dow, Phys. Rev. B Condens. Matter **42**(8), 5135 (1990).
30. A. E. Galashev, V. A. Polukhin, I. A. Izmodenov, and O. R. Rakhmanova, Glass Phys. Chem. **33**(1), 86 (2007).
31. S. Plimpton, J. Comput. Phys. **117**(1), 1 (1995).